International Conference on Applied Energy 2020
Dec. 1 - Dec. 10, 2020, Bangkok / Virtual
Paper ID:0220

An Automotive Fuel Cell-Lithium Battery Hybrid System Model Considering Detailed Heat and Mass Transport Processes

Yahan Xu, Zirong Yang, Yan Yin, Qing Du, Kui Jiao*
State Key Laboratory of Engines, Tianjin University, 135 Yaguan Rd, Tianjin, China, 300350
*Corresponding author: kjiao@tju.edu.cn; tel: +86-22-27404460; fax: +86-22-27383362

ABSTRACT

Most of existing fuel cell hybrid electric vehicle (FCHEV) powertrain models ignore the real physical processes such as heat and mass transfer, and the researches of individual power sources do not consider the whole vehicle level. A comprehensive transient FCHEV model is developed, including an integrated fuel cell system model, a one-dimensional transient $LiFePO_4$ battery model, and a vehicle dynamics model. A rule-based energy management strategy is developed, and simulations are carried out under China standard operating conditions of light vehicles. Output performances and dynamic responses of the hybrid power system are investigated. The results show that both fuel cell system and lithium battery can successfully work within a suitable range and simultaneously achieve good responsiveness.

Keywords: fuel cell, Li-ion battery, FCHEV, rule-based energy management strategy

1. INTRODUCTION

Proton exchange membrane fuel cell (PEMFC) has the advantages of rapid hydrogen refilling, high cruising range, high power density, and high energy conversion efficiency, making it an ideal choice of the automobile power system [1]. Dynamic operating conditions such as start-stop, variable load, and idle load severely reduce the durability and reliability of fuel cells [2]. Meanwhile, the transient performances are difficult to meet the power demand. Therefore, fuel cell hybrid electric vehicles (FCHEVs) equipped with auxiliary power sources can achieve faster responses to load changes, higher reliability, and longer cruising range.

Over the past few decades, many related researches have been carried out. For FCHEV powertrain simulation, the models are mostly simplified black box models or equivalent circuit models. Saman et al. [3] designed the powertrain elements of an FCHEV considering fuel cell system/battery/ultra-capacitor. The model was based on the simulation software ADVISOR platform. The energy management strategy (EMS) considering a novel power-sharing method and an intelligent control technique based on fuzzy logic control was developed.

Based on the zero-dimensional fuel cell and battery model, Zhang et al. [4] developed a FCHEV composed of 3 fuel cells and 1 storage battery, which improved the durability of the fuel cell through strategic energy management. These models ignore the electrochemical reactions, heat and mass transfer of fuel cells and Li-ion batteries such as the temperature changes of fuel cells and Li-ion batteries. Many researches have been conducted on individual power sources, such as Li-ion batteries or fuel cells. Jiao et al. [5] studied the effects of gas humidification during cold start processes through a three-dimensional multiphase transient model. In Li-ion battery simulation, Thomas and Newman et al. [6, 7] developed the well-known classical models and corresponding theories. These studies did not fully consider the entire power system and the inter-coupling of hybrid power sources. Therefore, it is necessary to develop a comprehensive FCHEV hybrid system model with consideration of detailed heat and mass transport processes.

In this study, a transient hybrid power system considering real physical processes is developed, including a comprehensive fuel cell system model, a transient Li-ion battery model, DC/DC converter model, and vehicle dynamics model. A rule-based energy management strategy is developed to investigate the transient responses of hybrid power system during China standard operating conditions of light vehicles.

2. MODEL DEVELOPMENT

The structure diagram of a typical FCHEV is shown in Figure 1a.

2.1 Fuel cell system model

In our previous research, the fuel cell system model has been developed and verified [8].

2.2 $LiFePO_4$ battery model

Figure 1b shows the structure of a lithium-ion battery, including positive current collector (PCC), positive electrode (P), separator (S), negative electrode (N), and negative current collector (NCC).

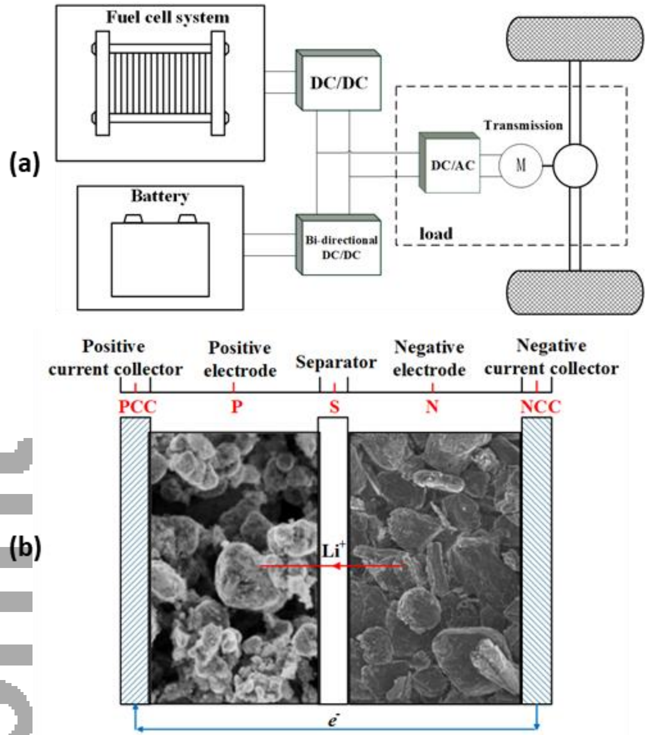

Fig 1 (a) Structure diagram of a typical FCHEV. (b) Schematic diagram of a lithium-ion battery

Temperature, lithium-ion concentration, and electric potential are solved in the corresponding computational domain. When solving the conservation equations, the explicit calculation method is adopted to improve the simulation efficiency and calculation stability. After discretization and transformation, the calculation formulas are expressed as:

$$\eta_i^t = \frac{RT_i^t}{0.5F}\operatorname{asinh}\left[\frac{j_i^t}{2k_{\text{eff},i}\sqrt{c_{e,i}^t(c_{s,i}^{\max}-c_{s,i}^{*,t})c_{s,i}^{*,t}}}\right] \tag{1}$$

$$c_{s,i}^{\text{ave},t+\Delta t} = c_{s,i}^{\text{ave},t} - \frac{3j_i^t\Delta t}{R_{p,i}} \tag{2}$$

$$c_{s,i}^{*,t} - c_{s,i}^{\text{ave},t} = -\frac{R_{p,i}j_i^t}{5D_{\text{eff},i}^s} \tag{3}$$

$$c_{e,i}^{t+\Delta t} = c_{e,i}^t + \frac{D_{\text{eff},i\_i+1}\Delta t}{\varepsilon_i l_i}\cdot\frac{c_{e,i+1}^t-c_{e,i}^t}{\frac{l_{i+1}+l_i}{2}} + \frac{a_i(1-t_+)j_i^t\Delta t}{\varepsilon_i} \tag{4}$$

$$-\kappa_{\text{eff},i\_i+1}\frac{\phi_{e,i+1}^t-\phi_{e,i}^t}{\frac{l_{i+1}+l_i}{2}} + \kappa_{\text{eff},i\_i+1}\frac{2(1-t_+)R}{F}\frac{T_{i\_i+1}^t}{c_{e,i\_i+1}^t}\cdot\frac{c_{e,i+1}^t-c_{e,i}^t}{\frac{l_{i+1}+l_i}{2}} = l_i a_i F j_i^t \tag{5}$$

$$T_i^{t+\Delta t} = T_i^t + \frac{\Delta t}{\rho_i C_{p,i} l_i}\left(\lambda_{i\_i+1}\frac{T_{i+1}^t-T_i^t}{\frac{l_{i+1}+l_i}{2}} - \lambda_{i-1\_i}\frac{T_i^t-T_{i-1}^t}{\frac{l_i+l_{i-1}}{2}}\right) + \frac{Q_{\text{source},i}\Delta t}{\rho_i C_{p,i}} \tag{6}$$

where *i, t, t+*$\triangle t$ are node location, last time step, next time step. The solid-phase average ion concentration in Eq. (2) and the solid-phase surface ion concentration in Eq. (3) are solved at the positive and negative electrodes, respectively. The liquid-phase ion concentration in Eq. (4) and the liquid-phase potential in Eq. (5) are solved at the battery positive, negative electrodes, and the separator. The temperature in Eq. (6) is solved at all five nodes. State of charge (SOC) is determined by the solid phase concentration of the negative electrode. The output voltage is obtained by subtracting the potential of the two collector plates. The coupling of other parameters and temperature is described by the Arrhenius formula.

$$SOC^t = \frac{1}{l_n c_{s,n}^{\max}}\int_0^{l_n} c_s^{\text{ave},t}dx \tag{7}$$

$$V_{out}^t = \phi_{s,pcc}^t - \phi_{s,ncc}^t = \eta_p^t + \phi_{e,p}^t + U_p - \left(\eta_n^t + \phi_{e,n}^t + U_n\right) \tag{8}$$

$$k_0 = k_{0,\text{ref}}\exp\left[\frac{E_{aR}}{R}\left(\frac{1}{T_{\text{ref}}} - \frac{1}{T}\right)\right] \tag{9}$$

2.3 Vehicle dynamics model

The load power of the vehicle dynamic model is calculated by the following formula:

$$P_{\text{load}} = \frac{\left(F_g + F_{roll} + F_{AD} + F_{acc}\right)v}{\eta_{tr}} \tag{10}$$

where

$$F_g = mg\sin\theta \tag{11}$$

$$F_r = k_r mg\cos\theta \tag{12}$$

$$F_{ad} = 0.5\rho k_{ad} A_f v^2 \tag{13}$$

$$F_{acc} = m\frac{dv}{dt} \tag{14}$$

2.4 DC/DC converter model

As shown in Figure 1a, there are boost DC/DC converters and bidirectional DC/DC converters in the system. This study assumes that the efficiency of the two converters is 95%.

3. RESULTS AND DISCUSSION

3.1 Model validation

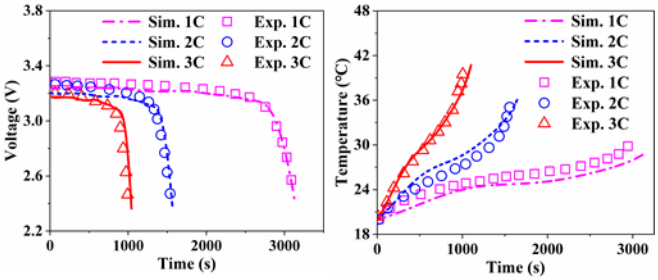

Fig 2 Comparison of voltage and temperature of lithium batteries under different discharge rates between simulation results and experimental data [3].

The fuel cell system model used in this paper has been verified for each component in our previous studies [8], and the subsequent calculations of fuel cell system parameters in this paper are consistent with previous studies. Figure 2 shows the comparison of simulation results and experimental test data [3] of the LiFePO4 model in 1C, 2C, 3C discharge rates. The model parameters in this paper are also set according to the literature [3]. Good agreement is observed.

3.2 Rule-based energy management strategy

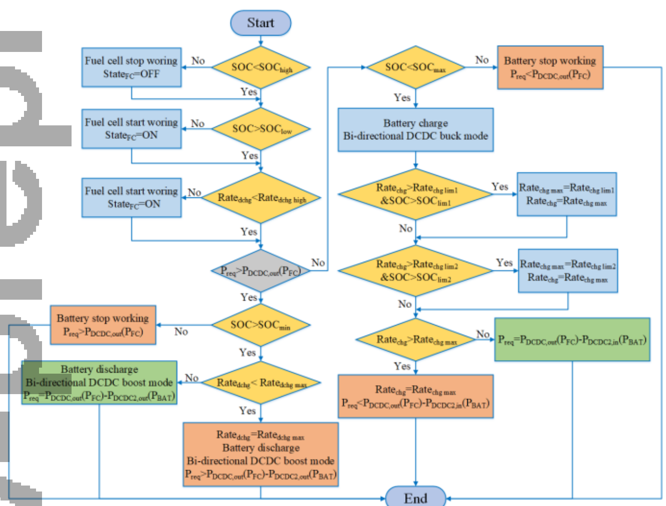

Fig 3 Rule-based energy management strategy

To verify the feasibility of the developed model in real road conditions, a rule-based energy management strategy is proposed. In this strategy, there are two states of the fuel cell system, on and off. The SOC of Li-ion battery varies within a fixed range. At high SOC, the charge rate of the lithium-ion battery to recover braking energy is limited, which avoids charging the Li-ion battery to reach the cut-off voltage too quickly. The detailed energy management strategy is shown in Figure 3. The constructed FCHEV includes a 30 kW fuel cell system and a 5.5 kWh $LiFePO_4$ battery. The car weighs 1.5 tons.

3.3 Results and discussion

The China standard operating conditions of light vehicles are adopted as road conditions. Figure 4a shows that the conditions are divided into three sections: low speed, medium speed, and high speed. The ambient temperature is 20°C, and the fuel cell operating temperature is controlled at 60°C. The corresponding hybrid system performances are shown in Figure 4b.

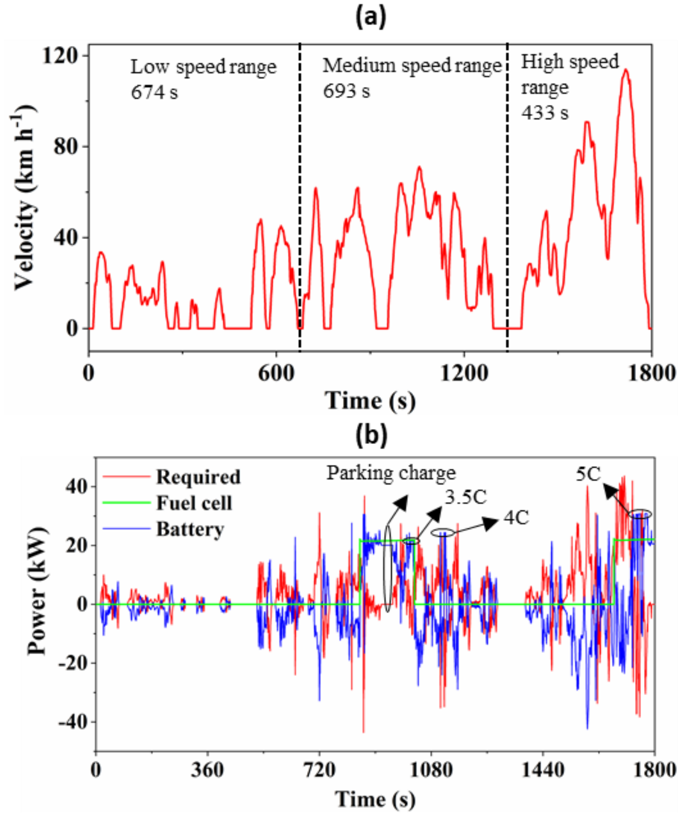

Fig 4 (a) The China standard operating conditions of light vehicles. (b) Hybrid system performances under the proposed EMS.

When the fuel cell is turned on, its power is preferentially supplied to the load. The Li-ion battery provides/absorbs the additional power. At low speed, power is provided by the Li-ion battery, and the energy efficiency is high. At medium speed, the fuel cell turns on for a while and then turns off. A parking charge and battery charge rate limit of 3.5C and 4C occurs in this process. During parking, the power generated by the fuel cell is recovered by the lithium-ion battery. At high speed, the fuel cell is turned on again. The battery charge rate reaches over 5C during this process. When the fuel cell is turned on, it is operated at a high-efficiency point while maintaining relatively stable operations. Further, the reliability and durability of the fuel cell are also improved.

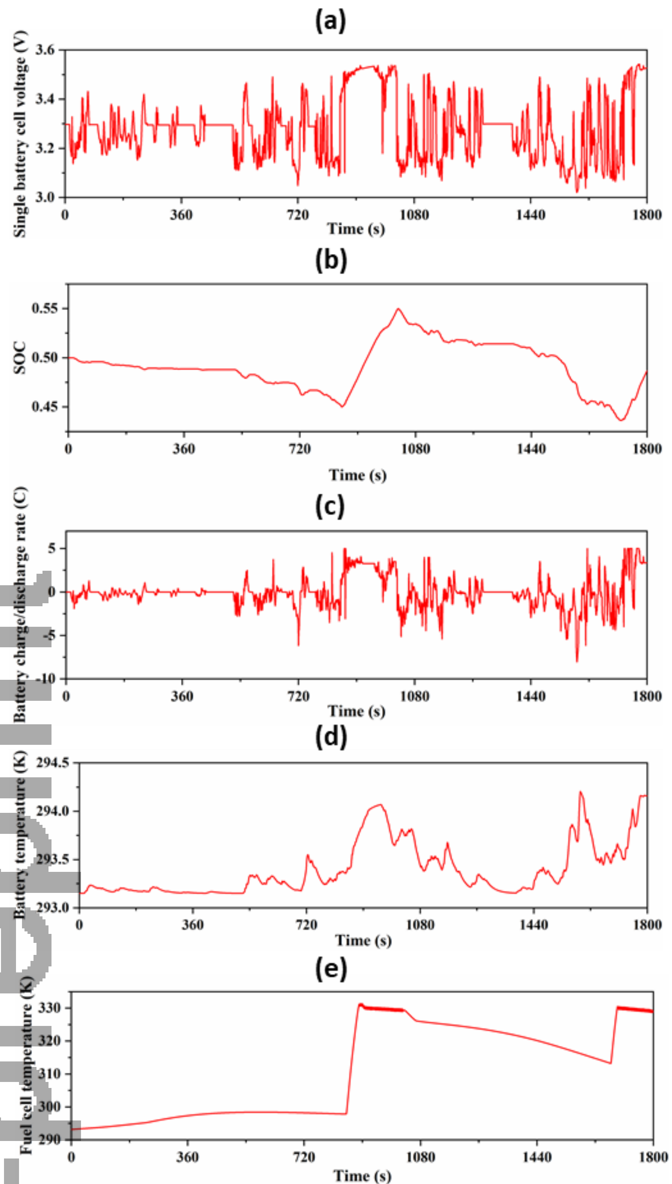

Fig 5 Fuel cell and li-ion battery parameter variations

Figure 5a shows the variations of single battery cell voltage, which remains within the safety range of 3 V to 3.55 V. Figure 5b shows that the SOC has remained between 0.45 and 0.55. Figure 5c shows that the charge/discharge rate of the cell remains mostly within 5C with peak discharge rate reaching 8C. Figure 5d shows that the cell temperature fluctuates below 295 K and rises rapidly after the fuel cell is turned on. Figure 5e shows that the temperature of fuel cell rises rapidly and stabilizes after turning on and falls slowly after turning off. From the above results, there is no excessive discharge rate, power loss and system overload occurring under China standard operating conditions of light vehicles. The developed energy management strategy enables both fuel cells and Li-ion batteries to operate under relatively stable conditions.

4. CONCLUSIONS

(1) A comprehensive transient FCHEV model considering the actual physical process of fuel cell and lithium battery is established. Both power source models have been compared with experimental data to verify the simulation accuracy. Output performances and dynamic responses of the hybrid power system are investigated.

(2) A rule-based energy management strategy has been developed under China standard operating conditions of light vehicles. The fuel cell and Li-ion battery are successfully operated under reasonably stable conditions. Meanwhile, transient responsiveness and energy efficiency are good.

ACKNOWLEDGEMENT

The study is supported by the National Key Research and Development Program of China (2018YFB0105601).

REFERENCES

[1] Jiao K, Li X. Water transport in polymer electrolyte membrane fuel cells. Progress in Energy and Combustion Science. 2011;37:221-91.

[2] Pei P, Chen H. Main factors affecting the lifetime of Proton Exchange Membrane fuel cells in vehicle applications: A review. Applied Energy. 2014;125:60-75.

[3] Ahmadi S, Bathaee SMT, Hosseinpour AH. Improving fuel economy and performance of a fuel-cell hybrid electric vehicle (fuel-cell, battery, and ultra-capacitor) using optimized energy management strategy. Energy Conversion and Management. 2018;160:74-84.

[4] Zhang H, Li X, Liu X, Yan J. Enhancing fuel cell durability for fuel cell plug-in hybrid electric vehicles through strategic power management. Applied Energy. 2019;241:483-90.

[5] Jiao K, Li X. Effects of various operating and initial conditions on cold start performance of polymer electrolyte membrane fuel cells. International Journal of Hydrogen Energy. 2009;34:8171-84.

[6] Doyle M. Modeling of Galvanostatic Charge and Discharge of the Lithium/Polymer/Insertion Cell. Journal of The Electrochemical Society. 1993;140:1526.

[7] Thomas KE, Newman J. Thermal modeling of porous insertion electrodes. Journal of the Electrochemical Society. 2003;150:A176-A92.

[8] Yang Z, Du Q, Jia Z, Yang C, Xuan J, Jiao K. A comprehensive proton exchange membrane fuel cell system model integrating various auxiliary subsystems. Applied Energy. 2019;256.